Near-field focusing with Sinusoidally Modulated Reactance Surfaces

I. Iliopoulos*, M. Esquius-Morote, M. Garcia-Vigueras, J. R. Mosig

Abstract
Leaky-wave antennas (LWA) have recently become a trending field of study at frequencies ranging from the microwave to the millimeter wave regime or even at optics. Key role in this interest plays their wide flexibility when it comes to beam forming. LWAs present vast advantages emerging from the fact that they can be single and easily fed, beam-scanning antennas. In the context of this work focusing is achieved using LWAs and specifically, implementing Sinusoidally Modulated Reactance Surfaces. To the authors' knowledge the resulting structures (designed originally at 15GHz, yet presenting inherent scalability), illustrate great focal characteristics at pioneering focusing distances.

Laboratory of Electromagnetics and Acoustics (LEMA), EPFL, Switzerland
***Corresponding author**: jiliopou@gmail.com

Introduction

LWA antenna theory has been well known for long, yet in recent years much effort has been put to connect theory with practice, resulting in numerous publications. Previous research [1] - [2] shows that near-field focusing is possible using LWAs, or as they are also known, leaky-wave lenses (LWL). In the current contribution we propose to investigate a circular aperture, implemented by meta-surfaces, which offers a sizeable improvement in the capability of controlling the characteristics of leaky waves.

In order to focus the near fields radiated by the antenna, a tapering procedure has to be applied, which consists in the modulation of the leaky wave propagation constant along the antenna length [3]. In particular, both the real (β) and the imaginary (α) parts of this constant should be independently tuned, in order to additionally obtain a amplitude taper and achieve higher aperture efficiency [4]. This tapering/modulation is achieved by properly modifying the antenna geometry.

Focusing inside the microwave regime takes place in the near-field or in the Fresnel region, where the fields have not yet acquired TEM characteristics, thus becoming a challenging regime to work at. A theorem from 1962 by Sherman [5] allows the designer to actually use far-field design techniques to setup Fresnel region focusing under a certain condition for the aperture phase distribution. In fact, this theory is very close to the ray model approach, which will be used in the context of this work.

The following study is constrained to apertures and relevant technologies, which exhibit the advantage of being low profile and high directivity structures. Table 1 summarizes the state of the art combined with former leaky-wave approaches. *Taper* stands for the aperture distribution capabilities of the technologies, while *Feed* for the feeding network and the type of the source (internal-external). To the author's best knowledge there is no literature entry for the proposed scheme, which combines all positive characteristics.

Table 1. Possible antenna candidates for near-field focusing

Antenna Type	Taper	Feed	Losses	Ref.
Arrays	√	X	X	[6, 7]
Phased Arrays	X	∼	√	[8, 9]
Reflect-arrays/ Fresnel Zone Plates	∼	X	√	[10, 11, 12, 13]
1D-Waveguide Mechanically Modulated LWA	X	X	X	[14]
2x1D-LWAs(Tx&Rx)	√	√	X	[15]
2D Spiral Slot LWA	√	√	√	[2, 16]
2D-Meta-surface (Sinus. Mod.)	√	√	√	-
RLSA	√	√	√	[17]

1. Near-field focusing with leaky-waves

1.1 Leaky waves over circular apertures

Let us consider a circular aperture situated at the x-y plane and fed at the center, on which a leaky-wave is propagating. In order to focus the radiation produced by this aperture at an arbitrary point above it, it is apparent that the leaky-waves of some area should be operating in the backward regime, thus pointing at negative angles related to the direction of propagation of the wave on the interface. In our approach the focus will be constrained at the z-axis. In order to achieve this, a periodic structure has to be used, able to support the propagation of higher order harmonics. The wavenumber of the -1 harmonic is given by [18]

$$\beta_{-1} = \beta_\rho - \frac{2\pi}{p} \tag{1}$$

where β_ρ is the wavenumber of the guided wave and p is the periodicity. By correctly adjusting the latter it is possible to excite leaky-waves radiating at a requested angle given as

$$\sin\theta_{rad} = \frac{\beta_{-1}}{k_0} = \frac{\beta_\rho - \frac{2\pi}{p}}{k_0} \tag{2}$$

where

$$-1 < \sin\theta_{rad} < 1 \tag{3}$$

thus allowing radiation towards negative angles (backwards). Special care has to be taken to avoid higher harmonics from entering the radiation regime, which would cause spurious radiation. Nevertheless, if the pointing angle is kept constant over the aperture, the result is the gathering of the electromagnetic energy at a specific angle in the far-field. This is the classical antenna scheme.

On the other hand, if the pointing angle (β_{-1} or p) is varied in an appropriate way it is possible to gather the electromagnetic energy at a specific point near the aperture. This is illustrated in fig. 1, which in other terms stands for the ray model, the validity and applicability of which in near-field focusing has been proven in [2].

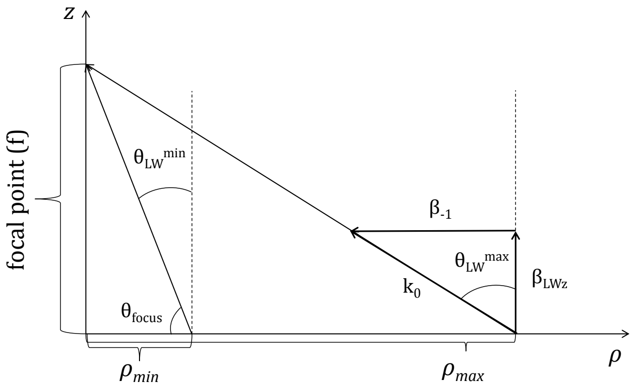

Figure 1. Ray-approach of focusing

Since the pointing angle is modulated over the aperture, the leaky phase constant becomes a function of the radius and angle (ρ and ϕ). In our approach, ϕ-symmetry is preserved and since the goal is to focus at a distance F on the axis of the aperture the result for the radiating harmonic[1] is

$$\beta_{LW}(\rho) \equiv \beta_{-1}(\rho) = -k_0 \sin^{-1}\left(\tan\frac{\rho}{F}\right) \tag{4}$$

Since leakage is present the wavenumber is complex, presenting a term α which is also a function of ρ, specifically

$$k(\rho) = \beta_{LW}(\rho) - j\alpha(\rho) \tag{5}$$

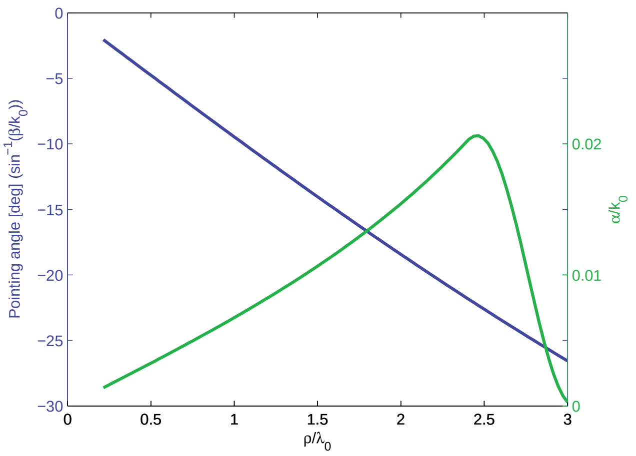

Figure 2. Leaky-wave parameters of a focused aperture at 2R$_0$

Concluding, the field over the aperture can be divided in two components, an amplitude and a phase one as

$$E(\rho) = A(\rho)e^{-j\Phi(\rho)} \tag{6}$$

where

$$A(\rho) = \sqrt{\frac{\alpha(\rho)\rho_{min}}{\rho}}\, e^{-\int_{\rho_{min}}^{\rho}\alpha(\rho)\,\mathrm{d}\rho} \qquad \text{and} \tag{7}$$

$$\Phi(\rho) = \int_{\rho_{min}}^{\rho} \beta_{LW}(\rho)\,\mathrm{d}\rho \tag{8}$$

It should be noted that the E-field presented above is in scalar form and the actual polarization will depend on the technology used. Using equation 7 it is possible to obtain the aperture efficiency which is given by

$$\eta_{APPeff}^{2D} = \frac{2}{\rho_{max}^2 - \rho_{min}^2}\int_{\rho_{min}}^{\rho_{max}} \bar{A}(\rho)\rho\,\mathrm{d}\rho \tag{9}$$

where $\bar{A}$ denotes normalized values. In order to realize a high aperture efficiency, it is apparent that a uniform aperture illumination is needed. It was shown in [19] that the aperture illumination function can be reversed and mapped to the leakage rate (α) using the following equation.

$$a(\rho) = \frac{\frac{1}{2}\rho A^2(\rho)}{\frac{1}{\eta_{RADeff}}\int_{\rho_{min}}^{\rho_{max}}\rho A^2(\rho)\,\mathrm{d}\rho - \int_{\rho_{min}}^{\rho}\rho A^2(\rho)\,\mathrm{d}\rho} \tag{10}$$

1.2 Focal Properties

By using the above principles, the leaky-wave parameters of an aperture focused at 2R$_0$ with quasi-uniform amplitude distribution (where R$_0$ is the radius of the structure) are illustrated in figure 2. Supposing that the aperture field is TM polarized,[2] it is possible to calculate the radiated near-fields

---

[1] Supposing that only the -1 harmonic is radiating

[2] This will be the case in this sinusoidally modulated reactance surface approach. In fact as of [20], the patches used, create an inductive surface, which only supports TM waves

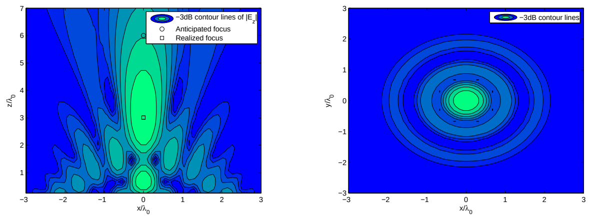

Figure 3. Power density contour plots (vertical and horizontal) of the E_z component of an aperture focused at $2R_0=6\lambda_0$

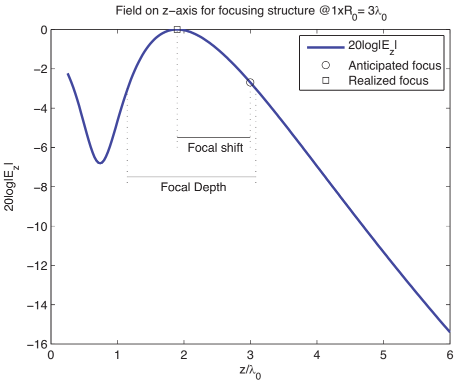

Figure 4. Focal characteristics

using classical electromagnetic theory [21, p. 284-286]. The radiated power density carried by the Ez[3] component of an aperture focused at $2R_0$ is shown in figure 3.

The axial power density of an aperture focused at $F=R_0$ is illustrated in figure 4, where we notice the focal figures of merit. The focus shift is a phenomenon that cannot be avoided and was described in [22]. Concerning the depth of focus (DoF), it is defined in [8] as *"the distance between the two points along the axis normal to the antenna's aperture (the z axis) where the power density is 3 dB below its maximum value"*. Another focal characteristic is the spot diameter, which can be seen in figure 3 and has a similar definition to the DoF, but in the horizontal sense.

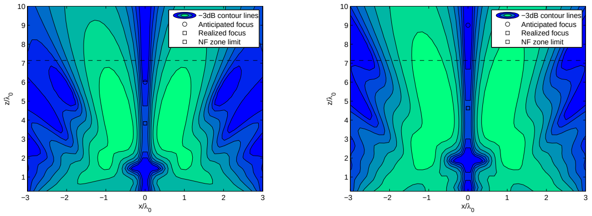

Figure 5. Near fields of E_ρ when focusing at 2 and 3 times the structures's radius

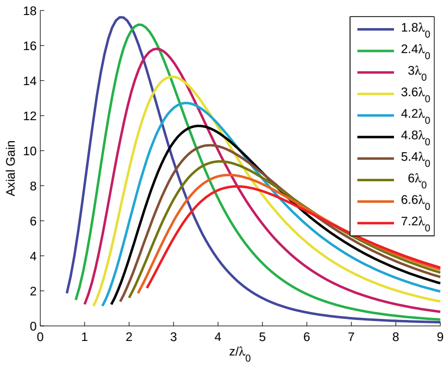

Figure 6. Axial gain for various foci

1.2.1 Focusing the z-component

The results presented so far, consider the E_z component of the focused field. This is a novelty by itself since to the author's knowledge all relevant focus schemes are focusing the tangential to the interface components. Nevertheless, the vertical component cannot be focused far from the structure since it cannot propagate, yet it offers a very concentrated field of great focal characteristics (low focal depth and spot diameter). This "lag" of the focus can be seen in figure 6. The axial gain which can be interpreted as the *focus gain* is calculated from [5] as

$$G=\frac{4\pi P}{W}, \tag{11}$$

where

$$P=\frac{1}{2}\sqrt{\frac{\varepsilon}{\mu}}z^2\left|E_{Axis}\right|^2 \qquad \text{and} \tag{12a}$$

$$W=\frac{1}{2}\sqrt{\frac{\varepsilon}{\mu}}E_0^2A \tag{12b}$$

We notice that apart from the increase of the focal shift, a deterioration of the gain is also present in further foci due to the spread of the field. An interesting remark concerns the E_ρ component, which follows more closely the anticipated focus (as of other publications [2]), yet is not focusing in our case due to the ϕ-symmetry. This is illustrated in figure 5. The focal depth is severely deteriorated.

1.3 Sinusoidally modulated reactance surfaces

Sinusoidally modulated reactance surfaces (SMRS) are based on the theory of Oliner et. al. [23] which has been lately explored extensively starting with [24]. The underlying concept is to map a sinusoidal modulation to a high impedance surface as

$$X(\rho)=X_s[1+M\cos(\frac{2\pi}{p}\rho)] \tag{13}$$

where X_s is the average surface reactance, M is the modulation index and p is the periodicity. It can be seen that this concept is linked with the holographic antenna theory [25]. Further

---

[3] The E_ρ component cannot be focused due to the symmetry of the structure, in fact it cancels out itself on the axis

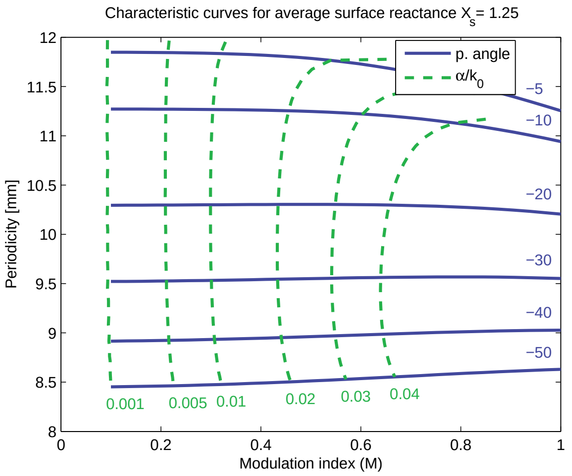

Figure 7. Design curves of SMRS for X_s=1.25 @15GHz

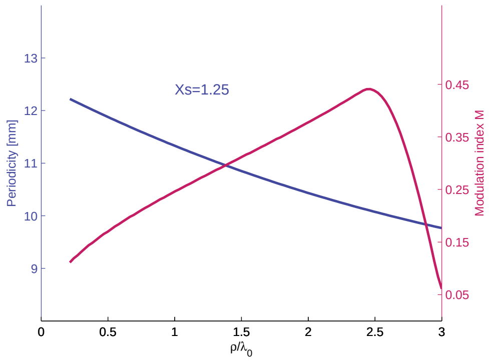

Figure 8. SMRS parameters

information on SMRS and a practical application can be found in [26].

In the context of this work a design graph is addressed in fig. 7 which illustrates the possibility of independently controlling the pointing angle and the leakage factor ($\beta \& \alpha$) of these structures, especially for modulation indexes lower than 0.6. In general, SMRS can inherently scan all elevation angles, from back to front endfire[4]. Using the equations governing the design graph of figure 7, it is possible to map leaky-wave parameters (fig. 2) to meta-surface ones, which are illustrated in figure 8. The average reactance X_s is set to $1.25\eta_0$ for matching purposes, where η_0 is the free space impedance.

In order to create the modulation of equation 13 one can use the meta-surface approach. Here we consider a patch configuration. In fig. 9 the geometry of the structure's cell is illustrated, accompanied by the relevant impedance for a TMM10 substrate (ϵ_r=9.2) of h=1.27mm. The minimum gap is defined by manufacturing constraints and in our case is 100μm. In general, higher cell sizes can provide higher impedances, up to the point that the patch itself starts resonating. Of course, larger cells degrade the surface resolution with a decent trade-off reaching 2mm.

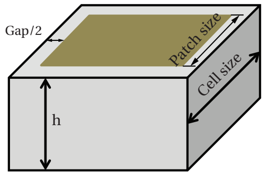

(a) Cell geometry

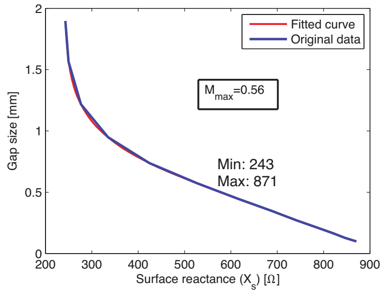

(b) Cell impedance for a cell size of 2mm

Figure 9. Cell geometry and the resulting surface impedance

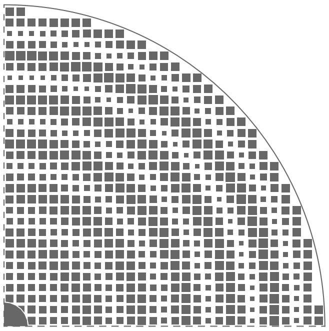

Figure 10. A quarter of the simulated surface.

2. Results and Discussion

In this section the theory presented previously is applied using the meta-surface technology at 15GHz. Full wave simulations using Ansoft HFSS present a decent match with the theoretical results.

2.1 Modeling and Results

A generic illustration of a meta-surface sector is depicted in figure 10. We can notice here both the change of the periodicity (change of pointing angle) and the change of the modulation index (aperture illumination tapering) along the length of the structure. The latter is apparent in the intensity of the variation of the size of adjacent patches. Higher variation denotes higher modulation index. The disk at the center of the structure serves the feed matching and its radius is set to 4.3mm. The structure is fed at the center using a conventional SMA connector.

Three models where designed and simulated using HFSS for three different foci; 1, 1.5 and 2 times the radius of the

---

[4] Broadside radiation is only possible if a certain asymmetry is introduced to the structure (e.g. spiral)

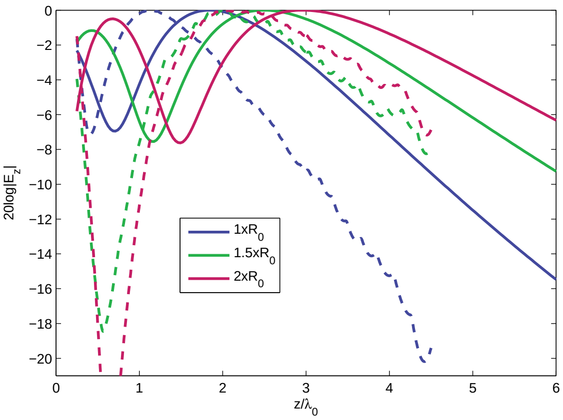

Figure 11. Comparison of leaky-wave theory (continuous lines) with meta-surface simulated with HFSS (dashed lines)

structure, which was set to $3\lambda_0$. Table 2 summarizes the obtained results, which show excellent focus properties. Focusing is very sharp both in the vertical (depth of focus) and horizontal direction (spot diameter) in all cases. Much sharper than the relative literature [2].

A comparison with theory can be seen in figure 11. The results follow the expected behavior ("lagging" of the focus at longer distances) and the deviation from theory is acceptable, taking into account the approximation of the leaky-wave theory and that the focus is extremely close to the structure.

Table 2. Summary of results for the three models

	1xR$_0$=3λ_0	**1.5xR$_0$=4.5λ_0**	**2xR$_0$=6λ_0**
Realized foc.	$1.125\lambda_0$	$2\lambda_0$	$2.4\lambda_0$
DoF	$1.3\lambda_0$	$1.9\lambda_0$	$2.13\lambda_0$
Spot diam.	$0.32\lambda_0$	$0.36\lambda_0$	$0.39\lambda_0$
Focus shift	$1.9\lambda_0$	$2.5\lambda_0$	$3.6\lambda_0$

2.2 Conclusions

In this report, Sinusoidally Modulated Reactance Surfaces (SMRS), constituted by square patches, were tuned to focus the provided electromagnetic energy to the near-field. The structures are easily fed by a simple probe while they combine a flat profile with the ease of manufacture and scalability. Aperture efficiency optimization was taken into account, leading to very satisfactory focal characteristics. Good agreement was observed between leaky-wave theory and simulation, while further experimentation will ultimately prove the concept. To the author's knowledge, it is the first time that focusing is achieved at so close to the structure distances.

References

[1] A. J. Martinez-Ros, J. L. Gomez-Tornero, F. J. Clemente-Fernandez, and J. Monzo-Cabrera. Microwave near-field focusing properties of width-tapered microstrip leaky-wave antenna. *IEEE Transactions on Antennas and Propagation*, 61(6):2981–2990, 2013.

[2] J. L. Gomez-Tornero, D. Blanco, E. Rajo-Iglesias, and N. Llombart. Holographic surface leaky-wave lenses with circularly-polarized focused near-fields; part i: Concept, design and analysis theory. *IEEE Transactions on Antennas and Propagation*, 61(7):3475–3485, 2013.

[3] G. Goussetis J. L. Gomez Tornero and Y. Jay Guo. Metasurfing substrate integrated waveguides to mold the radiation from leaky waves. In *PIERS Proceedings*.

[4] M. Garcia-Vigueras, P. DeLara-Guarch, J. L. Gomez-Tornero, R. Guzman-Quiros, and G. Goussetis. Efficiently illuminated broadside-directed 1d and 2d tapered fabry-perot leaky-wave antennas. In *6th European Conference on Antennas and Propagation (EUCAP)*, pages 247–251, 2012.

[5] J. Sherman III. Properties of focused apertures in the fresnel region. *IRE Transactions on Antennas and Propagation*, 10(4):399–408, 1962.

[6] S. Karimkashi and A. A. Kishk. Focused microstrip array antenna using a dolph-chebyshev near-field design. *IEEE Transactions on Antennas and Propagation*, 57(12):3813–3820, 2009.

[7] K. D. Stephan, J. B. Mead, D. M. Pozar, L. Wang, and J. A. Pearce. A near field focused microstrip array for a radiometric temperature sensor. *IEEE Transactions on Antennas and Propagation*, 55(4):1199–1203, 2007.

[8] A. Buffi, P. Nepa, and G. Manara. Design criteria for near-field-focused planar arrays. *IEEE Antennas and Propagation Magazine*, 54(1):40–50, 2012.

[9] A. Yarovoy, P. Lys, P. Aubry, T. Savelyev, and L. Ligthart. Near-field focusing within a uwb antenna array. In *First European Conference on Antennas and Propagation, 2006. EuCAP 2006.*, pages 1–6, 2006.

[10] J. A. Encinar. Design of two-layer printed reflectarrays using patches of variable size. *IEEE Transactions on Antennas and Propagation*, 49(10):1403–1410, 2001.

[11] S. Karimkashi and A. A. Kishk. Focusing properties of fresnel zone plate lens antennas in the near-field region. *IEEE Transactions on Antennas and Propagation*, 59(5):1481–1487, 2011.

[12] C. Hsi-Tseng, H. Tso-Ming, W. Nan-Nan, C. Hsi-Hsir, T. Chia, and P. Nepa. Design of a near-field focused reflectarray antenna for 2.4 ghz rfid reader applications. *IEEE Transactions on Antennas and Propagation*, 59(3):1013–1018, 2011.

[13] S. Ebadi, R. V. Gatti, L. Marcaccioli, and R. Sorrentino. Near field focusing in large reflectarray antennas using 1-bit digital phase shifters. In *European Microwave Conference, 2009. EuMC 2009.*, pages 1029–1032, 2009.

[14] I. Ohtera. Focusing properties of a microwave radiator utilizing a slotted rectangular waveguide. *IEEE Transactions on Antennas and Propagation*, 38(1):121–124, 1990.

[15] I.-H. Lin, C. Caloz, and T. Itoh. Near-field focusing by a nonuniform leaky-wave interface. *Microwave and Optical Technology Letters*, 44(5):416–418, 2005.

[16] J. L. Gomez-Tornero, D. Blanco, E. Rajo-Iglesias, and N. Llombart. Holographic surface leaky-wave lenses with circularly-polarized focused near-fields; part ii: Experiments and description of frequency steering of focal length. *IEEE Transactions on Antennas and Propagation*, 61(7):3486–3494, 2013.

[17] A. Mazzinghi, A. Freni, M. Balma, D. Devona, G. Guarnieri, G. Mauriello, and M. Albani. Bessel beam generation with a rlsa antenna. In *2013 21st International Conference on Applied Electromagnetics and Communications (ICECom)*, pages 1–4, 2013.

[18] C.A. Balanis. *Modern Antenna Handbook*. Wiley, 2008.

[19] M. Garcia-Vigueras, P. DeLara-Guarch, J. L. Gomez-Tornero, R. Guzman-Quiros, and G. Goussetis. Efficiently illuminated broadside-directed 1d and 2d tapered fabry-perot leaky-wave antennas. In *6th European Conference on Antennas and Propagation (EUCAP)*, pages 247–251, March 2012.

[20] Daniel F. Sievenpiper. Artificial impedance surfaces for antennas. In C. Balanis, editor, *Modern Antenna Handbook*, pages 737–777. John Wiley & Sons, Inc., 2008.

[21] Constantine A Balanis. *Advanced engineering electromagnetics*, volume 111. John Wiley & Sons, 2012.

[22] Y. Li and Emil Wolf. Focal shifts in diffracted converging spherical waves. *Optics Communications*, 39(4):211 – 215, 1981.

[23] A. A. Oliner and A. Hessel. Guided waves on sinusoidally-modulated reactance surfaces. *IRE Transactions on Antennas and Propagation*, 7(5):201–208, 1959.

[24] G. Minatti, F. Caminita, M. Casaletti, and S. Maci. Spiral leaky-wave antennas based on modulated surface impedance. *IEEE Transactions on Antennas and Propagation*, 59(12):4436–4444, 2011.

[25] B. H.Fong, J. S. Colburn, J. J. Ottusch, J. L. Visher, and D. F. Sievenpiper. Scalar and tensor holographic artificial impedance surfaces. *IEEE Transactions on Antennas and Propagation*, 58(10):3212–3221, Oct 2010.

[26] A. M. Patel and A. Grbic. A printed leaky-wave antenna based on a sinusoidally-modulated reactance surface. *IEEE Transactions on Antennas and Propagation*, 59(6):2087–2096, June 2011.